The role of chemical design on the performance of organic semiconductors

Hugo Bronstein[1], Christian B. Nielsen[2], Bob C. Schroeder[3] & Iain McCulloch[4,5,*]

1. Department of Chemistry, University of Cambridge, UK
2. School of Biological and Chemical Sciences, Queen Mary University of London, UK
3. Department of Chemistry, University College London, UK
4. Department of Chemistry, Imperial College London, UK
5. Physical Science and Engineering Division, King Abdullah University of Science and Technology, Kingdom of Saudi Arabia

*Email: i.mcculloch@imperial.ac.uk

Abstract | Organic semiconductors are solution-processable, lightweight and flexible, such that they are increasingly being used as the active layer in a wide range of new technologies. The versatility of synthetic organic chemistry enables the materials to be tuned such that they can be incorporated into biological sensors, wearable electronics, semi-transparent photovoltaics and flexible displays. These devices can be improved not only by developing their synthetic chemistry but also by improving the analytical and computational techniques that enable us to understand the factors that govern material properties. Judicious molecular design provides control of the semiconductor frontier molecular orbital energy distribution and guides the hierarchical assembly of organic semiconductors into functional films where we can control the properties and motion of charges and excited states. This Review describes how molecular design plays an integral role in developing organic semiconductors for electronic devices in present and emerging technologies.

[H1] Molecular orbital design considerations

The energies of frontier molecular orbitals and the distribution of the orbitals in a π-conjugated molecule play critical roles in intra- and intermolecular charge transport, light absorption/emission, charge injection/extraction/trapping and electrochemistry. This is true for organic small molecules and conjugated polymers alike. In each case, the energy of the highest occupied molecular orbital (HOMO) largely depends on the electron density and delocalization of the π electrons throughout a π-conjugated backbone. Substituents that donate electron density mesomerically (for example, lone pair donation from N, O or S heteroatoms) or inductively (for example, alkyl chains) can contribute to raising the HOMO energy E_{HOMO}, decreasing the solid-state ionization potential (IP, Box 1). Conversely electron-withdrawing groups, such as –F, –C(O)R or –C≡N groups, can act to lower both the HOMO and lowest unoccupied molecular orbital (LUMO) energy, leading to an increase in the solid-state electron affinity (EA).

BOX 1 | **Energy levels in an isolated organic molecule and a molecular crystal or polymer.**

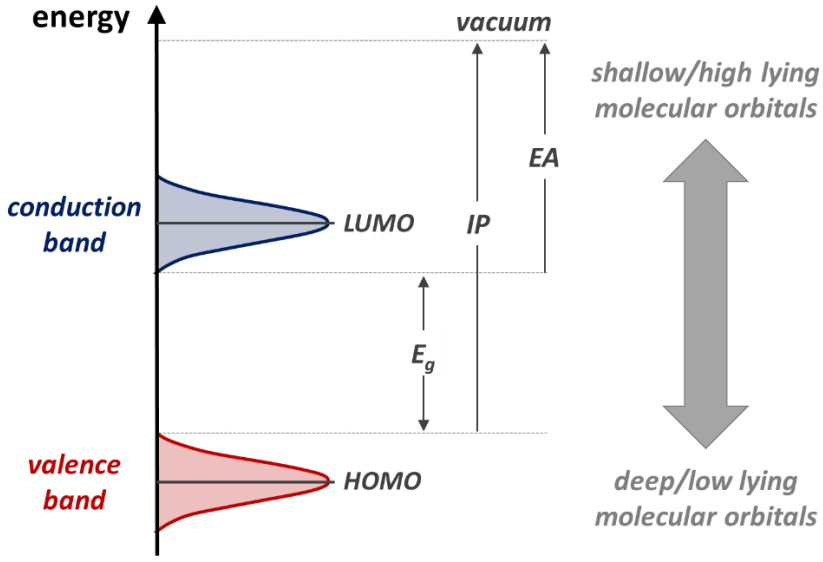

Isolated organic semiconductor moieties have discrete HOMO and LUMO energy levels, which are broadened into electronic bands — the valence and conduction band, respectively — when the moieties aggregate, either in terms of individual molecules in a solid state or moieties connected as part of a polymer. The optical band gap E_g is the difference in energy between the highest energy of the valence band and the lowest energy of the conduction band. The IP is the energy required to remove one electron from the top of the valence band, whereas the EA is the energy released by adding one electron from the vacuum level to the bottom of the conduction band.

The spatial distribution of a molecular orbital is important when considering intermolecular electronic coupling, which relies on efficient π-orbital overlap between two or more conjugated systems. The rational introduction of substituents into a conjugated organic molecule is a practical means to manipulate molecular orbital energies levels. (Fig. 1).

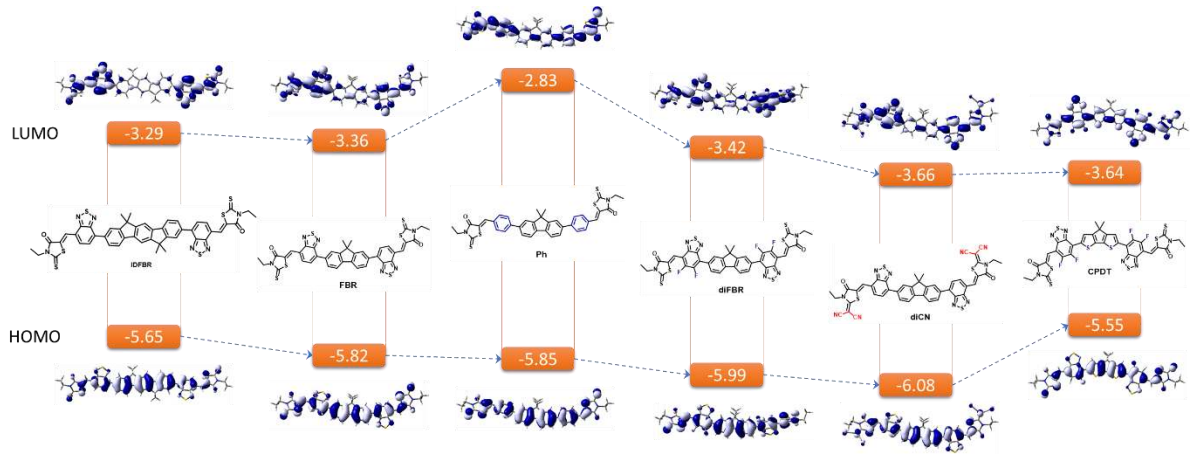

Figure 1 | **Manipulating frontier orbital distributions and energies.** A series of conjugated aryl molecules differing in aromatic units and substituent functionality is shown to exhibit contrasting distributions and energies of their highest occupied molecular orbital (HOMO) and lowest unoccupied molecular orbital (LUMO). Ground state geometries and HOMO wavefunction distributions were obtained using density functional theory with the B3LYP method and def2-SVP basis set, using Grimme's D3 dispersion correction and the BJ damping function. Time-dependent density functional theory, along with the ground state coordinates, was used at the same level of theory to calculate the LUMO wavefunction distributions.

As a starting point to illustrate "molecular engineering", (5*Z*,5′*Z*)-5,5′-(((6,6,12,12-tetramethyl-6,12-dihydroindeno[1,2-*b*]fluorene-2,8-diyl)bis(benzo[*c*][1,2,5]thiadiazole-7,4-diyl))bis(methanylylidene))bis(3-ethyl-2-thioxothiazolidin-4-one) (**IDFBR**, Fig. 1) was chosen. The HOMO wavefunction is delocalized over its entire π-conjugated backbone whereas in contrast, the LUMO wavefunction is predominantly localized on the electron-deficient 2,1,3-benzothiadiazole (BT) and rhodanine moieties.[1] In order to efficiently accept electrons from a light absorbing donor polymer, we are interested in tuning the LUMO energy of IDFBR, which is optimally achieved by the introduction of substituents at its periphery. To tune the HOMO energy however, we can add substituents at any conjugated part of the molecule. Replacing the central indenofluorene core with a smaller fluorene unit affords **FBR**, which has fewer delocalised electrons, resulting in an increase in HOMO energy (by almost 0.2 eV), with a smaller increase in the LUMO energy (less than 0.1 eV), due to the larger fraction of the conjugated unit having electron withdrawing functionality. A modification of **FBR** by replacing the BT units with a phenylene, results in **PH**, the LUMO energy of which is substantially higher lying (~0.5 eV) because the phenylenes are less electron-deficient (the HOMO is only marginally affected). Difluorinating the BT units in FBR gives **diFBR**, in which both the HOMO and LUMO energies are 0.1–0.2 eV lower lying on account of electron-withdrawing inductive effects of the electronegative F atoms. Another approach in the manipulation of the

molecular orbitals of FBR is to replace the C=S (thiocarbonyl) groups on the rhodanine periphery, with dicyanovinyl moieties, which are more strongly electron-withdrawing than the thiocarbonyl. Indeed, **diCN** has HOMO and LUMO energy levels that are ~0.3 eV lower than those of **FBR**. Both the electron density distribution along the molecule, as well as the delocalization of the π orbitals play a substantial role in determining the orbital energy levels. **FBR** has a non-planar backbone because the BT and fluorene units have neighbouring H atoms that participate in repulsive interactions. These steric effects can be alleviated by replacing the fluorene core with cyclopentadithiophene to give **CPDT**, a molecule with more π orbital overlap between rings, which contributes to both raising the HOMO energy and lowering the LUMO energy. The introduction of the electron-rich thiophene rings, further raises the HOMO energy. **CPDT** also exhibits electrostatic S···F interactions, with these electropositive and electronegative atoms, respectively, interacting to stabilise the planar backbone, affording additional raising of the HOMO energy and lowering of the LUMO energy. The greater π orbital delocalization means that the LUMO is now distributed further over the core of the molecule, and functionalization at any location within this region will affect the LUMO as well as the HOMO energy. Substituting the sp^3-hybridized C atom of the fluorene unit with either Si or Ge does not appear to influence either the HOMO or LUMO energies. This is surprising because incorporating larger heteroatoms between rings typically leads to a lengthening of the C–C bond linking the two aromatic rings, thereby attenuating the antibonding interactions that arise from the node of the HOMO between the rings and lowering the HOMO energy. Similarly, replacing the S atoms on the CPDT unit with other chalcogen atoms does not affect the electronic structure of CPDT. In general, having a larger chalcogen atom (E) in a ring lowers its aromatic character because the E–C bonds are longer, such that the chalcogen non-bonding valence electrons are less delocalized. The ring thus has more diene character, such that the overall molecule has a lower lying HOMO and a smaller bandgap[2].

Charge transport is sensitive to traps within the bulk,[3] and transport within p-type materials benefits from their low ionization potential, which makes the filling of deep traps thermodynamically unfavourable. Similarly, n-type materials benefit from a large EA, when again there are less accessible charge traps. Injecting holes from an electrode into the HOMO of a semiconductor is more energetically facile when the electrode workfunction is close to, or preferably larger than, the IP of the semiconductor. This allows for ohmic contact, with low contact resistance at the electrode–semiconductor interface. Correspondingly, for electron injection, the EA should be as large as possible. For an organic semiconductor device to be stable in operando, we must ensure that its neutral and charged forms do not participate in chemical reactions.[4] In order to prevent the most thermodynamically favourable reactions (those involving a combination of O_2 and H_2O), a neutral p-type semiconductor is predicted to require an ionization potential greater than 4.9 eV.[4] When this is not the case, the shallow HOMO semiconductor can, for example, reduce ambient O_2 in the presence of H_2O to form OH^-. Under operation, deep HOMO semiconductors can accept holes that can oxidise atmospheric H_2O. The activation barriers of these deleterious reactions fortunately lead to overpotentials that allow many organic semiconductors to perform redox slowly so they can exhibit reasonable shelf and operational stabilities. Electron transport is particularly affected by reactions with air, and it is essential to prevent the electron polaron from reducing ambient species. To accomplish this, the LUMO energy must be low enough to prevent excited electrons to reduce hydrated O_2 complexes to O_2^- (one of the most favourable electrochemical reactions)[5] or H_2O to OH^-. These unwanted electrochemical processes can lower charge transport and also lead to further irreversible reactions within a semiconductor. Defining a precise EA value that needs to be exceeded to prevent these redox reactions requires consideration of the overpotential of the reaction and device morphology. It has been proposed that organic molecules should have an EA greater than 4 eV to suppress oxidation reactions[6].

[H1] Organic field effect transistors

Charge transport in organic semiconducting polymers relies on a combination of intrachain polaron conjugation, facilitated by π-electron delocalization across the polymer backbone, and intermolecular charge-hopping between adjacent chains, facilitated by thin film microstructure. Charge carrier mobility is very sensitive to the nature of the close-packed hierarchical assembly of polymer backbones, which

can be optimized by tuning inter- and intramolecular interactions. Intermolecular contacts have been facilitated by many design motifs, including the μm-scale 3D ordering of poly{2,5-bis(3-alkylthiophen-2-yl)thieno[3,2-*b*]thiophene} (**pBTTT**, Fig. 2a) in thin films[7]. This material adopts a morphology in which ordered lamellar sheets of π-stacked conjugated **pBTTT** backbones exhibit out-of-plane order or "registration" directed by the interdigitation of vertically adjacent polymer chains. Interdigitation was made possible by the conformationally-tolerant, regular spacing of the side chains along the backbone, with optimal spatial separation to ensure an ordered and close-packed side chain density on interdigitation.

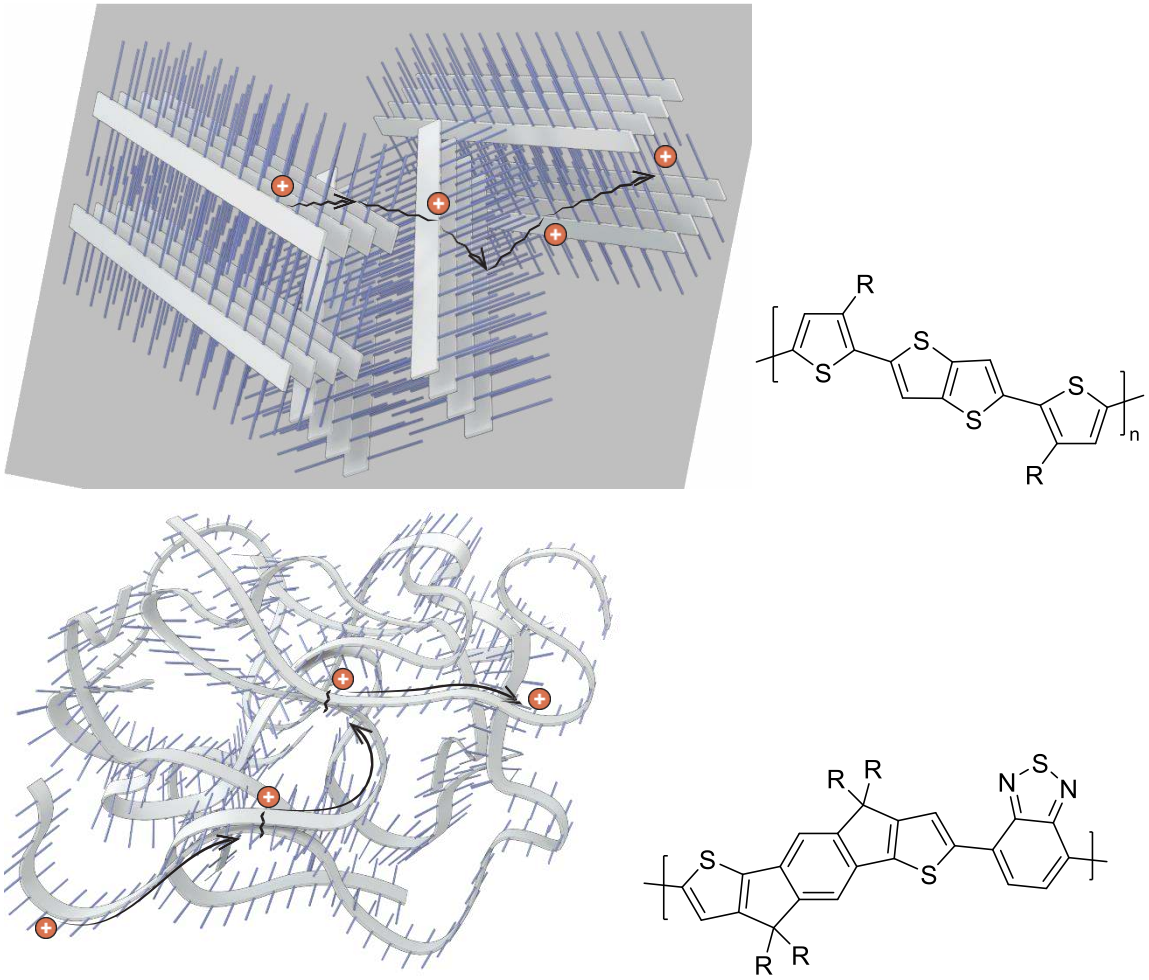

Fig. 2 | **Schematic illustrations and chemical structures of conjugated thiophene-derived polymers. a** | The 3D packing arrangement of **pBTTT** enables electron transport across and between its crystalline domains[7]. **b** | In contrast, **IDT-BT** exists as disordered chains, through which electrons can move[9]. The chains intermittently contact another chain or region, to/from which the electrons can move. The arrows illustrate a possible optimal pathway for electron transport. R represents alkyl side chains.

The approach of utilising non-covalent intermolecular interactions for charge transport optimisation, has subsequently been exploited in a series of isoindigo polymers[8], and a comparison drawn with similar associations observed in biology. Here the polymer alkyl side chains were described as undergoing 'molecular docking', the locking of side chains into voids along the polymer chain Indeed, the collective van der Waals interactions between inert aliphatic side chains are the dominant interaction that governs morphology and inter- and intrachain contacts. Even though the degree of interdigitation exhibited by **pBTTT** is extremely unusual, a close packed and regular alkyl distribution between backbones can act to not only order a material, but also minimize the local free volume such that unwanted species such

as H_2O are excluded. If these small molecules were included then they could participate in charge-trapping and lower carrier mobility.

Intramolecular charge transport can be optimally facilitated when the backbone of a polymer has the least possible amount of intrinsic energetic disorder, in which case it is resilient to torsional fluctuations between adjacent monomer units[9,10]. Energetic disorder is typically minimized by maximising the energetic barrier to rotation between aromatic repeat units along the backbone. Several design strategies can impart coplanarity of adjacent monomer units in a conjugated backbone. Non-covalent through-space interactions between adjacent rings can act as a barrier to rotation, thus promoting co-planarity. Common examples of this approach include the electrostatic attractions between heteroatoms in close proximity to the bond linking two aromatic rings in the backbone. The S atom on a linking thieno group, despite the presence of two lone pairs of electrons, presents a partially positive charge due to the donation of one lone pair to complete an aromatic ring. As a result, heteroatoms such as O and N, which have available lone pairs of electrons, can participate in strong attractive interactions with S, leading to a more rigid structure.[11-13] For example, in poly(3-alkoxythiophene) the S atom of one ring interacts with the more electronegative O atom in the adjacent ring (Fig. 3a). Other planarizing interactions include H-bonding interactions, which are observed between bis(lactam) building blocks and neighbouring residues. Thus, the crystal structures of small-molecule diketopyrrolopyrrole (**DPP**) and isoindigo derivatives feature O···H–C interactions.[14,15] The O atom in the electron-deficient lactam core interactions with a proximal H atom to lower rotational disorder and maximize π-orbital overlap between the rings. This concept can be extended to polymers by incorporating DPP and isoindigo monomers into the polymer backbone (Fig. 3a).

Non-covalent interactions can also be exploited to design highly coplanar copolymers with low energetic disorder such as the copolymer poly(indacenodithiophene-*co*-benzothiadiazole) (**IDT-BT**, Fig. 2b)[9]. The dominant planarising interaction in this case is a non-traditional H-bond between the N atom of the benzothiadiazole and the α-H atom of the adjacent indacenodithiophene. These strong N···H–C interactions outweigh the repulsive steric exchange energies associated with planarity, giving rise to extremely low energetic disorder in this polymer. Despite the high coplanarity, the polymer exhibits a hierarchical structure resembling a curved ribbon, and disordered over larger length scales, but the assembly of side chains promotes intermittent short contacts along the backbone. Thus, although charge is primarily transported in 1D along the backbone, there are occasional hops between chains such that these short contact polymers exhibit very high carrier mobilities.

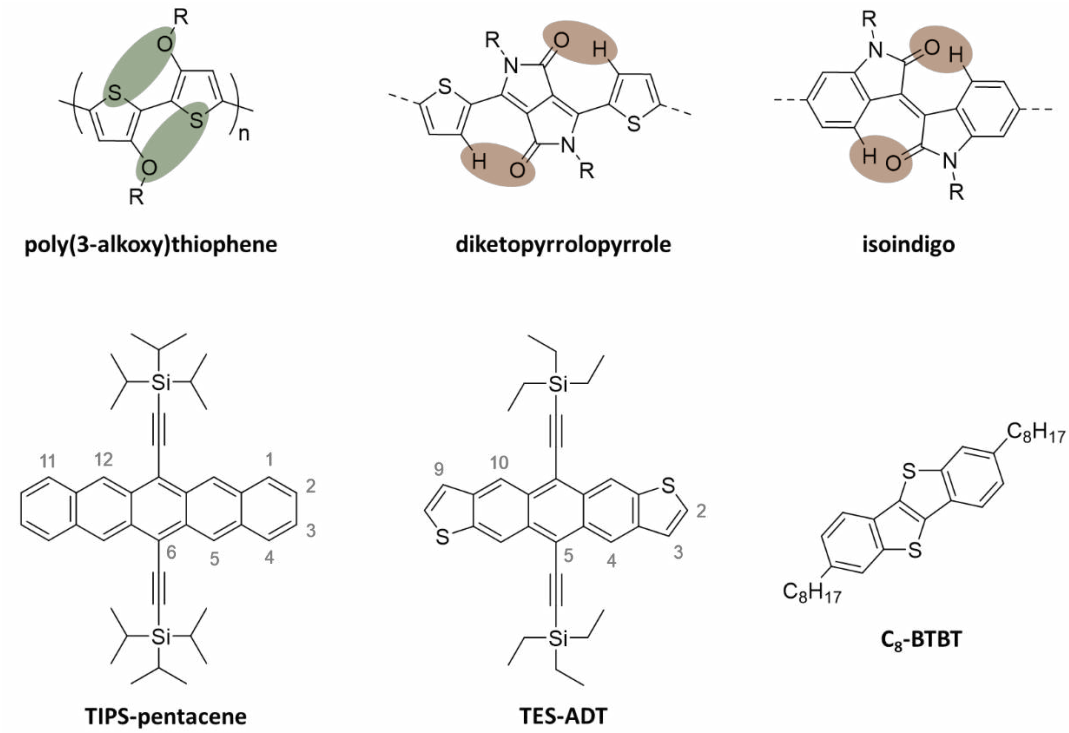

Fig. 3 | **Species that may find applications in organic field effect transistors. a** | Chemical structures of poly(3-alkoxy)thiophene, diketopyrrolopyrrole and isoindigo, with attractive planarizing interactions highlighted in green and orange. **b** | Chemical structures of high-performance molecular polyaromatic semiconductors **TIPS-pentacene**, **TES-ADT** and **C_8-BTBT**. R depicts alkyl side groups.

The above discussion has described organic polymers for charge transport, but small molecule semiconductors can also serve the same purpose in electronic devices. However, transport properties have been notoriously difficult to optimise through rational design at the molecular level. Crystal packing motifs play a dominant role and are extremely sensitive to even the smallest molecular perturbations. The herringbone and 2D slip-stack arrangements in particular have the required combination of electronic coupling and sufficient isotropy for efficient charge propagation. Two key building blocks have emerged as exemplary aromatic cores: pentacene (and its analogue anthradithiophene (ADT)) and benzothienobenzothiophene (BTBT). The packing motifs of these semiconducting molecules have been manipulated by strategically introducing substituents either on the central core (in the case of pentacene and ADT) or periphery (in the case of BTBT). Both pentacene and ADT can be readily functionalized, with the 6 and 13 positions of pentacene[16] and 5 and 11 positions of ADT being the most conveniently substituted. In this way, one can prepare species such as the bis((trialkylsilyl)ethynyl) derivatives **TIPS-pentacene** and **TES-ADT** (Fig. 3b). Introducing the –C≡C–SiR_3 groups increases solubility in organic solvents, blocks a possible site of oxidative degradation, and also adds a structural template that promotes 2D interdigitated π-stacking. This morphology is favourable in that it can give rise to thin films with higher charge carrier mobilities than most other packing motifs. Replacing the ^{i}Pr groups in **TIPS-pentacene** with Et groups changes the preferred packing structure to a lamellar 1D slip stack with a much larger charge transport anisotropy. Over the length scale of a transistor device, this leads to much lower charge carrier mobilities. In the case of **TES-ADT**, the inclusion of a peripheral F atom can promote short non-covalent contacts, further enhancing electronic coupling and, consequently, carrier mobility. BTBT has been identified as a suitable aromatic core for charge transport and is most easily substituted at the 2 and 7 positions, for example with linear $^{n}C_8H_{17}$ chains[17]. These chains increase solubility in organic solvents and have a highly calamitic (rod-like) shape that makes **C_8-BTBT** adopt a favourable herringbone packing motif. The short contacts between the conjugated cores of adjacent molecules in the crystal give rise to excellent and relatively isotropic electronic coupling, thus enhancing charge carrier mobility. Historically, the charge carrier mobilities observed in small molecule films have been larger than those in polymer films, and this has been attributed to the former having a lower energetic disorder, narrower

density of states, and fewer defects. However, the performances of semiconducting polymers with short intermolecular contacts are catching up, and they generally exhibit lower charge transport anisotropy, which makes them potentially favourable for integrated circuitry.

[H1] Organic photovoltaics

An organic photovoltaic (OPV) device includes a photoactive layer consisting of an electron donor and an electron acceptor. Both these materials can be tailored on a molecular level such that they absorb a large proportion of incident solar irradiation. An appropriate energetic offset between frontier orbitals of the donor and acceptor enables the splitting of excitons into free charge carriers, which can be collected at the separate electrodes. To absorb a large fraction of incident photons, an active layer substantially thicker than the exciton diffusion length is required, which, in turn, necessitates an intermixed donor:acceptor bulk heterojunction (BHJ, FIG. 4a) morphology.[18-20] Optimizing frontier molecular orbital energies of the donor and acceptor to increase the energetic driving force for charge separation and open circuit voltage (V_{oc}) must be balanced against efficient light absorption. Additionally, the donor:acceptor heterojunction must be judiciously controlled throughout the active layer to ensure efficient charge separation and collection with a high degree of morphological stability.

We now describe selected pairs of organic donor (FIG. 4b) and acceptor materials (FIG. 4c) in the context of a BHJ. In the extensively studied **P3HT**:**PCBM** heterojunction the LUMO energy levels are ~−3.2 and −4.2 eV for **P3HT** and **PCBM**, respectively, providing a large energetic offset to overcome the **P3HT** exciton binding energy (typically 0.3 eV) and drive charge separation through a Channel-I mechanism (Fig. 4a).This driving force, combined with the strong visible light absorption of **P3HT** and the favourable intermixed morphology of the BHJ, means that OPV devices can have power conversion efficiencies over 4%.[21]

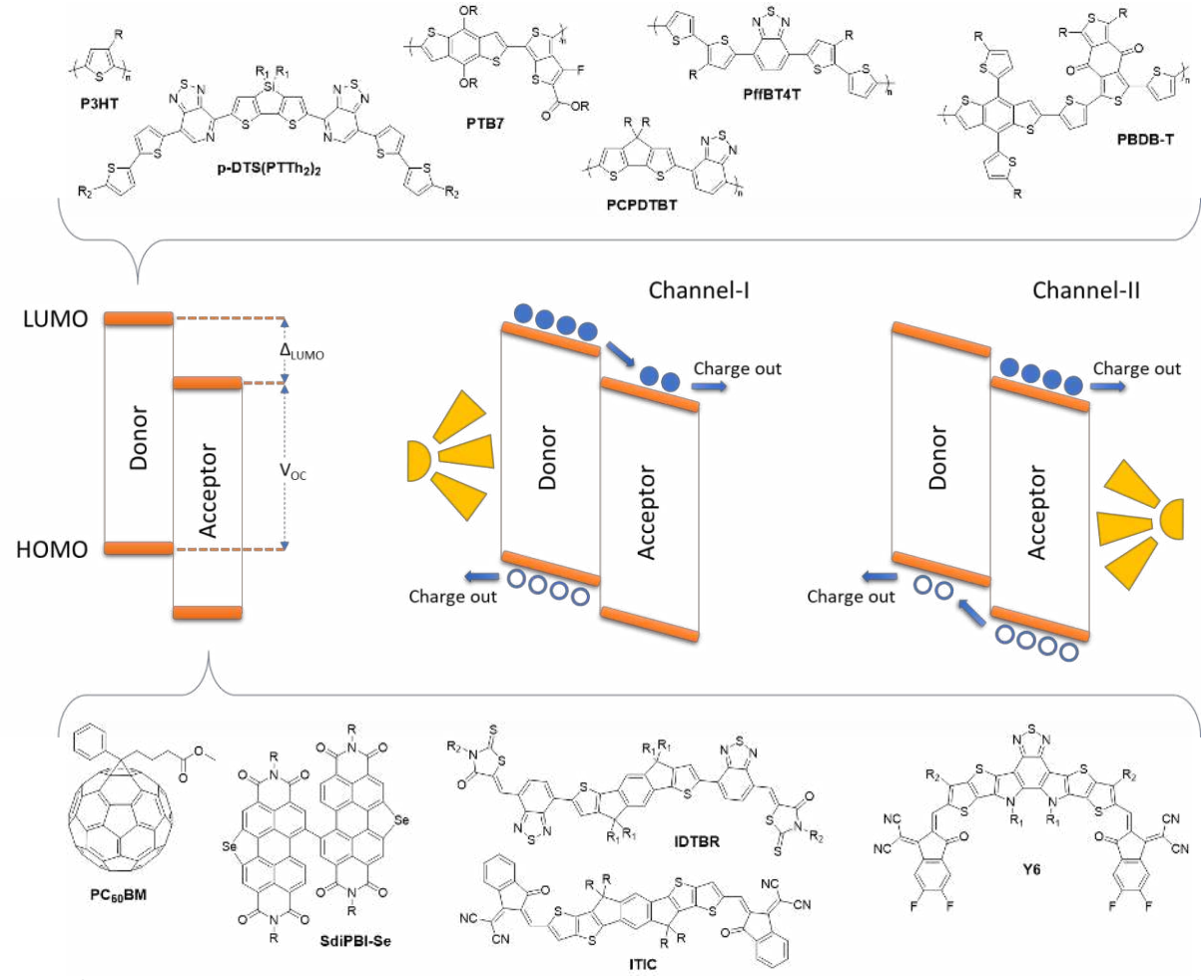

Fig. 4 | **Donor:acceptor bulk heterojunctions and some typical semiconducting components. a** | Energy diagrams depicting the donor–acceptor electronic band alignment and photocurrent generation

through a channel-I or II mechanism. **b** | Archetypical electron donors, which evolved from the early poly(3-hexylthiophene) P3HT to the more elaborate structures on the right. **c** | Archetypical electron acceptors. R describes solubilising side groups, such as linear and branched alkyl chains.

To harvest a greater proportion of the solar spectrum, OPV research rapidly shifted from using **P3HT** to instead designing electron donors with hybridized molecular orbitals from having alternating π-conjugated electron-rich and electron-poor repeat units. This effective and highly modular paradigm has been employed repeatedly to narrow the HOMO–LUMO gap and develop vast numbers of push–pull-type polymers with hybridized molecular orbitals. While a narrower-bandgap donor will absorb a greater proportion of the incoming photons and thus increase the extracted current (J_{sc}), it can compromise either the V_{oc} (shallower donor HOMO leading to smaller $LUMO_{acceptor}$–$HOMO_{donor}$ gap) or the charge separation (deeper donor LUMO leading to smaller $LUMO_{donor}$–$LUMO_{acceptor}$ offset) according to Figure 4a. Computational modelling suggests that the compromise between high voltage and efficient light absorption is best negotiated in a **$PC_{60}BM$**-based device using a donor material with a band gap around 1.5 eV.[22,23] One such material is **PCPDTBT**, which, despite having a near ideal band gap, performed poorly in bulk heterojunction devices. However, in 2007, the efficiency of a **PCPDTBT**:**$PC_{70}BM$** device was nearly doubled from 2.8 to 5.5% by adding a small amount of 1,8-octanedithiol when casting the active layer.[24] The dithiol preferentially improves the solubility of one of the photoactive components during film casting, enabling the bulk heterojunction morphology to be optimized and hence facilitating more reliable assessment of new photoactive materials without performance being overshadowed by poor morphology. Thus, by using push–pull-type narrow-bandgap donor polymers in conjunction with fullerene-based acceptors, the field steadily developed to being able to fabricate OPV devices with efficiencies up to ~11%. The donor materials often featured the non-covalent interactions discussed above, which promote polymer aggregation and facilitate phase separation on the exciton diffusion lengthscale.[25] From a frontier molecular orbital perspective, the HOMO energies of polymers such as **PTB7** (−5.15 eV), **PTB7-Th** (−5.24 eV) and **PffBT4T** (−5.34 eV) have been lowered to improve V_{oc}, while the bandgap has been increased slightly to ~1.6 eV. It should be noted that most high-performing PCBM devices are prepared not with **$PC_{60}BM$** as the acceptor, but using the C_{70} derivative **$PC_{70}BM$**, the lower symmetry of which allows stronger visible light absorption and greater channel-II photocurrent generation (Fig. 4a).[26]

Polymeric electron donors have dominated the OPV landscape, but there are some notable small-molecule electron donors. The pyridalthiadiazole-based small molecule **p-DTS(PTTh$_2$)$_2$** (Fig. 4b; E_{LUMO} = −3.6 eV; E_{HOMO} = −5.2 eV) absorbs in the broad 500–800 nm region and has a large LUMO–LUMO offset when paired with **$PC_{70}BM$**.[27] Controlling the blend morphology in a two molecule blend is challenging, as evidenced by the performance of **p-DTS(PTTh$_2$)$_2$**:**$PC_{70}BM$** devices being remarkable sensitive to processing conditions. A 70:30 donor:acceptor weight ratio with 0.25% solvent additive affords a power conversion efficiency of 6.7%. Small deviations from this composition see the performance drop precipitously.

The difference between the optical energy gap and the observed open-circuit voltage V_{oc} is referred to as the V_{oc} loss. This quantity is substantial for fullerene-based OPV devices that predominantly operate by a channel-I mechanism. Losses in high-performance PCBM cells are typically on the order of 0.8 eV — a value substantially larger than the exciton binding energy.[28] Using a non-fullerene acceptor (NFA) addresses this crucial barrier to further improving OPV device efficiencies. Although it is relatively straightforward to design and synthesise NFAs with appropriate HOMO and LUMO energy levels, early work highlighted the difficulties achieving both an intermixed blend morphology and sufficiently high charge carrier mobilities. For example, the high crystallinity of rylene diimides can preclude blending but has been mitigated by using twisted dimer-type acceptor structures. Indeed, the Se-annulated PDI motif in **SdiPBI-Se** can be used to achieve a PCE of 8.4%, and the four-blade propeller-type structure **FTTB-PDI4** gives rise to a higher PCE of 10.6% with a low V_{oc} loss of 0.53 V.[29,30] NFAs are more tunable than fullerenes in terms of frontier orbital energies, with SdiPBI-Se (E_{LUMO} = −3.9 eV; E_g = 2.2 eV) and **FTTB-PDI4** (E_{LUMO} = −3.6 eV; E_g = 1.9 eV) being two notable examples. The acceptor strength can be adjusted to match the chosen donor material, and E_g can likewise be tuned to ensure complementary absorption with the donor. The control over frontier orbital energies of NFAs is further

emphasized when one notes that their HOMOs and LUMOs are often spatially separated (FIG. 1), meaning that they can be adjusted independently of each other through molecular design. Additionally, NFAs typically have better light absorption than fullerene acceptors, and combined with the efficient hole transfer from acceptor to donor, this provides high channel-II photocurrent generation and high J_{sc} values.

A recently developed NFA design is a calamitic π-conjugated molecule with a central fused electron-rich (hetero)aromatic core flanked by terminal electron-deficient units such as indanedione or rhodanine. Further modularity in the molecular design can be incorporated by introducing electron-rich or electron-deficient π-conjugated spacers between the core and the flanking groups. **IDTBR** (FIG. 4c), which features an indacenodithiophene core flanked on each side by 2,1,3-benzothiadiazole and rhodanine, is one such calamitic acceptor.[31] The aromatic groups in its backbone are coplanar, such that **IDTBR** has a relatively narrow E_g (1.6 eV) and a **P3HT**:**IDTBR** active layer consequently absorbs strongly over the entire visible spectrum to give devices with efficiencies above 6%. In addition to improving the OPV performance of a simple and commercially scalable polymer such as **P3HT**, this result also illustrates that NFAs can be used as the primary low-bandgap light absorber, a role which was hitherto reserved for the donor material. Further improvements towards 8% power conversion efficiency with **IDTBR** has been reported for ternary blends using two complementary NFAs in conjunction with **P3HT**.[32] Further, **IDTBR** has an electronic structure (E_{LUMO} = −3.9 eV) that is compatible, in terms of LUMO–LUMO offset, with donor polymers such as **PffBT4T**. Indeed, a **PffBT4T**:**IDTBR**-based device can exhibit a power conversion efficiency of 10% and a very small V_{oc} loss (~0.5 V).[33] **ITIC** is another calamitic acceptor with comparable frontier orbital energy levels to those of **IDTBR**.[34] Likewise, **ITIC** has been used in several high-efficiency OPV devices, but as with **IDTBR** its optical bandgap ($E_g \approx 1.6$ eV) is comparable to most high-performing donor polymers developed specifically for fullerene-based devices. Thus, to absorb more broadly within the solar spectrum and increase J_{sc} it is beneficial to widen the bandgap of the donor polymer, so as to prevent a large spectral overlap with the NFA and possibly open a pathway for Förster energy transfer from the donor to acceptor. For example, **PBDB-T** (FIG. 4b, E_{HOMO} = −5.3 eV; $E_g \approx 1.8$ eV) comprises the weakly electron-deficient benzodithiophenedione unit in conjunction with the well-known electron-rich benzodithiophene motif. Being highly compatible with **ITIC**, this wider bandgap donor has been incorporated into devices, and the power conversion efficiencies of **PBDB-T**:**ITIC** active layers have gradually improved to over 14%.[35,36] **PBDB-T** has been modified by replacing alkyl chains with thioalkyls, as well as by fluorination and chlorination. Similarly, **ITIC** has been fluorinated and chlorinated — modifications that make it a better electron acceptor by lowering both the HOMO and the LUMO. The bandgap is slightly narrowed because the lowering is greater for the LUMO, on account of it being more distributed over the ITIC unit. This red-shifted absorption increases the J_{sc} while enhanced intra- and intermolecular interactions concurrently improve the extinction coefficient and charge-transport properties. Thus, the HOMO for the dichlorinated derivative **PBDB-T-2Cl** is 0.2 eV lower than that of **PBDB-T**, which makes the former useful in terms of affording OPV devices with high V_{oc} values with the active layer having good oxidative stability on account of the low-lying frontier orbital energies.

Most recently, the research community has looked beyond linear calamitic motifs to the curved structure **Y6**, a narrow bandgap NFA that absorbs strongly beyond 900 nm.[37] The central π-conjugated chromophore in this material is a 2,1,3-benzothiadiazole flanked by thieno[3,2-*b*]thiophene units that are fused onto the benzothiadiazole with *N*-alkylpyrrolo groups. The two alkyl side chains face each other and their interactions give **Y6** its slight twist (~17°), which ensures good solubility and favourable control of aggregation. This electron acceptor, paired with a fluorinated derivative of **PBDB-T** as the donor, can afford devices with power conversion efficiencies exceeding 15% and V_{oc} values above 0.8 V. The already small V_{oc} loss for this system can be further improved by using a chlorinated analogue of **Y6**, giving devices with efficiency above 16% and V_{oc} loss of only 0.53 V.[38] It is hypothesised that the much larger dipole moments in these bent NFAs compared to ITIC-type NFAs, and high electron mobility, contribute to the efficient charge separation and the fill factors around 75% — a high value that is desirable.

The tunability of molecular structure and frontier orbital energies has driven the OPV field over the last decade and related design approaches are being explored to sensitise other PV applications. This is most notable in the development of singlet fission materials that convert one high-energy singlet exciton to two lower energy triplet excitons. In turn, these triplets can generate additional e^-–h^+ pairs, for example, in low bandgap Si-based PV devices. With an S_1 singlet exciton energy of 2.4 eV, tetracene can absorb high-energy photons that would otherwise lead to high thermalization losses in Si cells, with subsequent singlet fission converting the singlet exciton into two triplet excitons. The T_1 triplet exciton energy of tetracene (~1.25 eV) nicely matches the bandgap of Si (1.1 eV). Although it is challenging to efficiently transfer the triplet excitons to the Si cell, this technology holds promise to exceed the Shockley–Queisser limit of 29% efficiency for a single junction PV device.

[H1] Organic light-emitting diodes

Despite organic light emitting diodes (OLEDs) being at an advanced stage of commercialization, their study remains an extremely active area of research in which many fascinating developments have been reported over the last 5–10 years. The fundamental operating principle of an OLED is extremely simple: charges injected from electrodes recombine within an organic layer to form an excited state which decays radiatively. However, spin statistics dictate that recombination of free charges results in a 1:3 ratio of singlet and triplet excited states being generated. The vast majority of OLED research has been targeted at overcoming the non-emissive nature of triplet excited states, a problem that would limit internal quantum efficiency (IQE) to 25% — the fraction of excites states that are singlets. The first successful approach to overcoming this was to move away from fluorescent emitters (1st generation materials, FIG. 4) to phosphorescent compounds (2nd generation). These compounds can emit quickly because they feature heavy metals, which promote intersystem crossing (ISC) of the triplets, as observed for organoplatinum and -iridium complexes (Fig. 4). This allowed all of the electrically generated excited states to be used radiatively such that devices with 100% internal quantum efficiency (with a maximum of 20–25% external quantum efficiency (EQE) due to outcoupling losses) could be prepared. However, problems associated with colour purity and stability (particularly in the blue region) have motivated the development of better OLED materials. The newest OLED materials (3rd generation) exhibit reverse intersystem crossing (rISC) to use triplet states. By lowering the energy gap between the lowest excited singlet and triplet states (ΔE_{ST}), the system has enough thermal energy to undergo rISC and have its triplet state convert into an emissive singlet. This process has fittingly been referred to as thermally-activated delayed fluorescence (TADF) and is a contemporary research topic of intense interest.

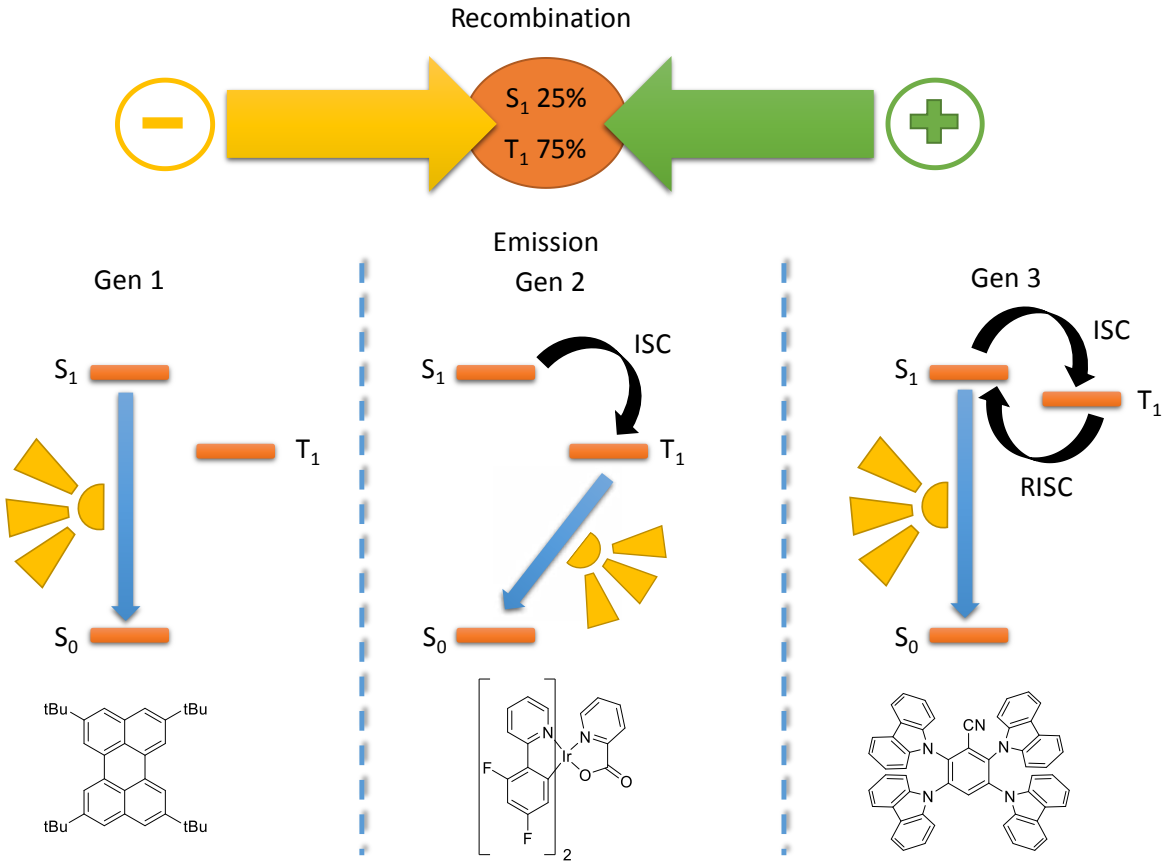

Fig. 4 | **Evolution of OLED emitters** Gen 1: Fluorescence, Gen 2: Phosphorescence, Gen 3: Thermally Activated Delayed Fluorescence

The most commonly used phosphorescent emitters are cyclometallated Ir(III) complexes dispersed within an organic host. It has long been known that the emitting dipole orientation of a dye influences the outcoupling efficiency (EQE/IQE) of OLEDs.[39] Despite this, the dipole orientations of phosphoresecent dopants have not been studied extensively, presumably due to the lack of any obvious driving force for alignment in (typically amorphous) host materials. However, a recent study using angle-dependent polarized photoluminescence emission spectroscopy shows that certain Ir complexes can be aligned in films.[40,41] The inherent asymmetry at the surface of a growing film apparently promotes dopant alignment in these otherwise amorphous films. Alongside other investigations into controlling phosphor alignment, external quantum efficiencies in excess of 30% have been reported, and it is projected that efficiencies of up to 60% are possible.[39,42] Despite decades of research, new strategies for achieving efficient blue emission from Ir complexes are still being sought with very impressive results emerging recently. Isomerizing a UV-emitting *N*-heterocyclic carbene complex of Ir(III) from its *fac* to *mer* form subtly red-shifts its emission such that it exhibits efficient deep blue phosphorescence with ~80% photoluminescence quantum yield (PLQY) and EQE ~15%.[43] There has recently also been considerable progress in the development of Ir-free phosphorescent emitters, including a new class of cyclometalated Au(III) complexes with tuneable emission spanning sky-blue to red. When deposited as thin films, these materials exhibited high PLQY values of up to 80%, and the OLEDs have excellent stability while maintaining EQEs up to 22%.[37] An extremely active area of research is the development of near-infrared OLED emitters for security and communication applications. Examples of $\{Pt^{II}[3\text{-(pyrazinyl)pyrazolato}]_2\}$ derivatives emit at 740 nm with a PLQY of 81%, and adopts a highly preferred horizontal dipole orientation such that its OLED devices exhibited an external quantum efficiency of 24%.[44] The origin of the near-infrared emission has been attributed to the stacking of Pt(II) centres on top of each other in the solid state, enabling metal–metal-to-ligand charge transfer.

Almost certainly the biggest development in OLED research over the last 10 years has been the observation of TADF from purely organic dyes. This work was pioneered by the group of Adachi, whose seminal publication described a series of purely organic materials such as 2,3,5,6-tetra(N-carbazolyl)benzonitrile (Fig. 4) that afford tuneable emission with high PLQYs and OLED EQEs approaching 20%.[45] This work showed that the simple design concept of spatially separating a molecule's HOMO and LUMO by using a twisted donor–acceptor structure lowers the energy gap between the first excited singlet and triplet states. Thus, triplet states can convert into emissive singlets by rISC, such that the materials exhibit TADF. By tuning the number, twist angle and electron density of donor moieties linked to the acceptor(s), one can obtain a series of compounds that collectively exhibit extremely high PLQY and OLED EQEs from the blue to near infrared.[46,47,48,49,50] Despite these impressive results, the exact mechanism by which rISC and TADF occur remains the subject of debate. In order to design efficient TADF emitters it is vital to consider both locally excited (LE) and charge-transfer (CT) states.[51] However, the process by which singlet and triplet states interconvert is not clear. 'Hidden' n–π mixed states may play an important role in the process or it is also possible that second-order vibronic coupling between the various excited states is required.[52-54] The role of intermediate electronic states that mediate the spin-flip through molecular vibrations has been demonstrated using a new model that also complements the notion of non-adiabatic coupling of triplet states promoting ISC.[55] Therefore, the synthetic strategy of merely minimising the S_1–T_1 energy gap requires refinement. One of the issues with conventional TADF is the requirement of donor–acceptor structures to be highly twisted, which results in broad spectral emission with low oscillator strength. This can potentially be overcome using a "hyperfluoresence" strategy, whereby a fluorescent guest is introduced into a TADF host, albeit at the expense of device simplicity.[56] It has also been suggested that a 'multi-resonant' strategy, that aims to spatially separate the HOMO and LUMO of a single planar molecule, can afford narrow ΔE_{ST} materials with high oscillator strengths and narrow emission.[57,58] Indeed, extremely impressive results using this strategy has recently been reported with a blue (469 nm) organoboron TADF-based OLED with an EQE of 34%.[59]

TADF has also been observed in organometallic systems, with [$Cu^{I}(NR_2)$(N-heterocyclic carbene)] complexes exhibiting outstanding optoelectronics properties (PLQY = 100%, EQE >25%).[60,61] Emission in these systems appears to stem from interligand charge-transfer states and, importantly, it appears that (as has also been suggested for organic TADF emitters[62]) that there is considerable spin-mixing, further indicating that the spin-pure picture of TADF emitters may be simplistic. However, as with phosphoresecent OLED emitters, achieving highly stable blue OLEDs with good colour purity has proved extremely challenging.

[H1] Beyond the state-of-the-art

A typical chemical design approach to optimize a semiconductor involves taking the conjugated aromatic units comprising the core or backbone and introducing systematic variations to isolate and study substituent effects on both morphology and frontier molecular orbitals. The results for the new materials are often compared to those in previous publications to justify a new design. In transistor research, unreliable charge carrier mobility values, extracted from invalid model equations and assumptions, have inflated expectations. Moreover, they have led to incorrect structure–property relationships being proposed, with molecular design conclusions reached on tenuous evaluations. This body of erroneous and misleading literature has seriously impeded progress in the development of materials for transistor applications. However, there are some obvious opportunities for further exploration. Incorporating aliphatic chains in these materials is primarily done to impart organosolubility, with a secondary reason being to control the solid-state structure. However, both alkyl chain and lamellar crystallization can come at the expense of conjugated backbone planarity and crystallinity. It is imperative that new semiconductors are designed in a holistic fashion, whereby the self-assembly of the system works with optimum performance rather than against it. It may be possible to deploy side chains in creative new ways to suppress undesirable phonon modes, which have recently been shown to severely affect charge transport.[63] Alternatively, removing the alkyl chains altogether should fundamentally improve charge transport. Detaching the side chains in situ, without compromising microstructural order, would increase backbone densification and performance. Although promising in principle, most methods to remove the chains do so at the expense of order ,

thereby detracting from transport properties. Molecular order has proved to be key in optimising charge transport, so finding ways to further reduce disorder in conjugated systems, or otherwise designing materials with a higher tolerance towards rotational fluctuations, will be essential to improve charge transport. To date, the introduction of labile side chains has proven challenging as it is difficult to predict the solid state packing of molecules and the different vibrational modes associated with a particular unit cell. With improvements in computational power, we have access to material property predictions that are more sophisticated and accurate, such that they can provide important insights into material packing motifs and phonon coupling modes. Thus, not only can we often calculate the many phonon coupling modes in a conjugated system, but, importantly, we can predict and identify the modes most detrimental to charge transport.

Besides the transport of electronic charge through a solid, other phenomena such as mixed conduction — electronic and ionic charge transport — are also attracting increasing attention due to their potential applications in biological interfacing.[64,65] In this context, an organic electrochemical transistor (OECT), a three-terminal device that can be gated through an aqueous electrolyte, is emerging as a powerful tool for bioelectronic applications. In an OECT, the active layer exhibits both electronic and ionic mobility throughout the bulk. Development of n- and p-type semiconducting polymers for OECTs therefore necessitates new design rules for tuning the frontier orbitals. For stable operation in aqueous environments, as a first prerequisite, the HOMO of p-type materials must be electrochemically accessible — at a potential lower than that at which H_2O oxidation would take place (1.23 V versus the normal hydrogen electrode). High-performance mixed conductors have much shallower HOMO levels, with E_{HOMO} between −4.4 and −4.6 eV, depending on the measurement technique.[66,67] HOMO levels in this energy range can be obtained with glycolated polythiophenes similar to poly(3-alkoxythiophene) (FIG. 3), in which the O atoms mesomerically donate electron density to the polymer backbone while the polar nature of the oligoether side chain facilitates ion transport. The development of n-type semiconductors is essential to sense biologically-relevant metabolites and cations, such as Na^+, K^+ and Ca^{2+}. To be operationally stable in H_2O, the main challenge centres around stabilizing the radical anion forms of the semiconductor towards H_2O and/or O_2.[68] This stability would dictate materials to have $E_{LUMO} < -4.0$ eV.[69,70] At present, the performance of electron-transporting OECT semiconductors lags substantially behind their hole-transporting counterparts. This lag has been tentatively attributed to coulombic charge-pinning from counterions, charge-trapping from H_2O, and other phenomena. Clearly, new molecular designs for electron transport in aqueous environments are required to overcome these limitations.

To develop organic semiconductors for photovoltaic applications, focus should not be on optimising the electronic and solid-state properties of a single material, but rather on understanding how to deliberately control the morphology of an active layer. This might entail, for example, incorporating multiple materials that are chosen to set up an energy cascade with large CT state energies. While the frontier orbital energy levels and the isolated molecular packing of both donor and acceptor can in general be controlled, there is presently a lack in understanding how functionalization of an organic molecule will affect its solid morphology on microscopic and macroscopic length scales. Using less-diffusive NFAs does help the morphological stability of a BHJ blend but it would be highly advantageous if the tertiary structure could be controlled to a greater extent, for instance by choice of heteroatoms, functional groups and side chains. Ideally, such approaches should also provide a means to 1) generate much thicker photoactive layers without unwanted vertical phase separation and excessive charge recombination and 2) scale up the cell's active area more effortlessly to generate large devices for beneficial practical implications. Over much shorter length scales, being able to control the donor:acceptor interfaces in the blend, for instance through molecular shape and dipole moments, would allow for greater understanding and control of the energy-transfer and charge-transfer processes. Another important aspect that requires further attention is the role of the CT state, how the CT state can be manipulated through chemical design and how this can be used to suppress recombination processes. Recent work indicates that electrostatic potential mapping, for instance, could be a useful and rapid tool to help understand how molecular structure and intermolecular interactions influence the charge separation processes.[71] The recent reports describing **Y6**, a curved NFA structure markedly different from the previous best NFA performers in terms of molecular design, have to a large extent taken the

OPV community by surprise. This promising example shows that there is still ample room to improve device performance, and also highlights the lack of unified molecular design criteria. Detailed structure–property relationships of NFAs and the main reasons for their excellent performance continue to be explored. Factors such as their off-axis dipoles, high electron mobilities, facile energy transfer processes and potential for good Förster energy overlap with donors could play important roles. As the OPV research community now embarks on in-depth fundamental studies of devices based on **Y6** and its analogues, further pieces of this puzzle will emerge. This insight will push the device performance closer towards the 20% efficiency mark and hopefully add to the understanding of molecular and frontier energy level design criteria.

The commercialization of OLED technologies has already been a monumental success. However, we lack a detailed understanding of the exact photophysical processes at play during charge recombination and emission. Moreover, we require a clear relationship between chemical structure and photophysical properties to rationally design new materials and realize progress. It is necessary to further understand the origin of the stability/instability of excited states, in particular in the presence of charges. Identifying degradation pathways may allow us to come up with chemical modifications enhance the stability of emitters. Despite this, present generations of OLED materials are operating close to their theoretical maxima and for a step-change in performance, a new generation of materials must be developed. Some encouraging signs of emerging 4th generation materials that warrant exploration are emerging. For example, there have been recent reports of extremely efficient OLED devices based on radical fluorophores.[72,73] These compounds, which feature the well-known luminescent tris(2,4,6-trichlorophenyl)methyl (TTM) radical motif, emit from a doublet excited state such that recombination is independent of the excited state spin. However, thus far these materials have only exhibited electroluminescence in the red/near-infrared and it remains to be seen whether it is possible to tune them to cover the entire visible spectrum. Another interesting new approach involves the use of host materials that can undergo singlet fission, which, in principle, could allow for IQEs of 200%.[74] Yet, such a device fashioned using the emitter [Er^{III}(8-hydroxyquinolinato)$_3$] as the guest in a rubrene singlet fission host gave a very low EQE, likely due to the low PLQY of the Er(III) complex. Thus, in order for this strategy to succeed it will be necessary to not only develop wide band-gap singlet fission hosts but also highly emissive near-infrared emitters capable of harvesting triplet excitons. There have been several recent reports of OLEDs that exploit triplet fusion, whereby two triplets annihilate and produce an emissive singlet.[75-77] Although this limits IQE to a maximum of 50% (if only triplets are injected), it could allow for low driving voltages and may offer blue emitters with greater photostability than present compounds.

There is a need to improve the chemistry used to synthesize organic semiconductors. The presence of (often hard to detect) residual impurities can result in batch-to-batch variations or unintentional doping. The availability and compatibility of chemical building blocks dictates the choice of reactions used in synthetic routes. For example, polymerizations often rely on Pd-catalysed cross-couplings, such as the Yamamoto, Suzuki–Miyaura, and Stille reactions. Although these coupling are extremely efficient, their low atom economy and requirement (in the case of the present polyaromatic substrates) for chlorinated solvents does not comply with sustainability requirements. Further, these reactions are not particularly suitable for large-scale production. C–H activation and condensation chemistry circumvent some of these problems by shortening the synthetic pathway and making extensive functionalization of monomers obsolete.[78] The narrow scope and restrictions on what building blocks are accessible leave ample room for improvement. Developing new chemical polymerisation protocols that allow for control over molecular weight and polydispersity whilst reducing chemical defects (that might occur on, for example, homocoupling or partial oxidation) will be an integral to advance the quality of synthesised materials.

[H1] References

1 Holliday, S. *et al.* A rhodanine flanked nonfullerene acceptor for solution-processed organic photovoltaics. *J. Am. Chem. Soc.* **137**, 898–904 (2015).

2 Planells, M., Schroeder, B. C. & McCulloch, I. Effect of chalcogen atom substitution on the optoelectronic properties in cyclopentadithiophene polymers. *Macromolecules* **47**, 5889–5894 (2014).

3 Nikolka, M. *et al.* High operational and environmental stability of high-mobility conjugated polymer field-effect transistors through the use of molecular additives. *Nat. Mater.* **16**, 356–362 (2016).

4 de Leeuw, D. M., Simenon, M. M. J., Brown, A. R. & Einerhand, R. E. F. Stability of n-type doped conducting polymers and consequences for polymeric microelectronic devices. *Synth. Met.* **87**, 53–59 (1997).

5 Abbaszadeh, D. *et al.* Electron trapping in conjugated polymers. *Chem. Mater.* **31**, 6380−6386 (2019).

6 Usta, H. *et al.* Design, synthesis, and characterization of ladder-type molecules and polymers. air-stable, solution-processable *n*-channel and ambipolar semiconductors for thin-film transistors via experiment and theory. *J. Am. Chem. Soc.* **131**, 5586–5608 (2009).

7 McCulloch, I. *et al.* Liquid-crystalline semiconducting polymers with high charge-carrier mobility. *Nat. Mater.* **5**, 328–333 (2006).

8 Lei, T. *et al.* Systematic investigation of isoindigo-based polymeric field-effect transistors: design strategy and impact of polymer symmetry and backbone curvature. *Chem. Mater.* **24**, 1762–1770 (2012).

9 Venkateshvaran, D. *et al.* Approaching disorder-free transport in high-mobility conjugated polymers. *Nature* **515**, 384–388 (2014).

10 Lemaur, V. *et al.* Resilience to conformational fluctuations controls energetic disorder in conjugated polymer materials: insights from atomistic simulations. *Chem. Mater.* **31**, 6889–6899 (2019).

11 Nielsen, C. B., White, A. J. P. & McCulloch, I. Effect of fluorination of 2,1,3-benzothiadiazole. *J. Org. Chem.* **80**, 5045–5048 (2015).

12 Conboy, G. *et al.* To bend or not to bend — are heteroatom interactions within conjugated molecules effective in dictating conformation and planarity? *Mater. Horiz.* **3**, 333–339 (2016).

13 Thorley, K. J. & McCulloch, I. Why are S–F and S–O non-covalent interactions stabilising? *J. Mater. Chem. C* **6**, 12413–12421 (2018).

14 von Eller-Pandraud, H. Structure cristalline de l'isoindigo. *Acta Cryst.* **13**, 936–938 (1960).

15 Naik, M. A., Venkatramaiah, N., Kanimozhi, C. & Patil, S. Influence of side-chain on structural order and photophysical properties in thiophene based diketopyrrolopyrroles: a systematic study. *J. Phys. Chem. C* **116**, 26128–26137 (2012).

16 Anthony, J. E., Brooks, J. S., Eaton, D. L. & Parkin, S. R. Functionalized pentacene: improved electronic properties from control of solid-state order. *J. Am. Chem. Soc.* **123**, 9482–9483 (2001).

17 Ebata, H. *et al.* Highly soluble [1]benzothieno[3,2-*b*]benzothiophene (BTBT) derivatives for high-performance, solution-processed organic field-effect transistors. *J. Am. Chem. Soc.* **129**, 15732–15733 (2007).

18 Sariciftci, N. S., Smilowitz, L., Heeger, A. J. & Wudl, F. Photoinduced electron transfer from a conducting polymer to buckminsterfullerene. *Science* **258**, 1474–1476 (1992).

19 Yu, G., Gao, J., Hummelen, J. C., Wudl, F. & Heeger, A. J. Polymer photovoltaic cells: enhanced efficiencies via a network of internal donor–acceptor heterojunctions. *Science* **270**, 1789–1791 (1995).

20 Tamai, Y., Ohkita, H., Benten, H. & Ito, S. Exciton diffusion in conjugated polymers: from fundamental understanding to improvement in photovoltaic conversion efficiency. *J Phys Chem. Lett.* **6**, 3417–3428 (2015).

21 Kim, Y. *et al.* A strong regioregularity effect in self-organizing conjugated polymer films and high-efficiency polythiophene:fullerene solar cells. *Nat. Mater.* **5**, 197–203 (2006).

22 Scharber, M. C. *et al.* Design rules for donors in bulk-heterojunction solar cells — towards 10 % energy-conversion efficiency. *Adv. Mater.* **18**, 789–794 (2006).

23 Kirkpatrick, J. *et al.* A systematic approach to the design optimization of light-absorbing indenofluorene polymers for organic photovoltaics. *Adv. Energy Mater.* **2**, 260–265 (2012).

24 Peet, J. *et al.* Efficiency enhancement in low-bandgap polymer solar cells by processing with alkane dithiols. *Nat. Mater.* **6**, 497–500 (2007).

25 Liu, Y. *et al.* Aggregation and morphology control enables multiple cases of high-efficiency polymer solar cells. *Nat. Commun.* **5**, 5293 (2014).

26 Dimitrov, S. D. *et al.* Towards optimisation of photocurrent from fullerene excitons in organic solar cells. *Energy Environ. Sci.* **7**, 1037–1043 (2014).

27 Sun, Y. *et al.* Solution-processed small-molecule solar cells with 6.7% efficiency. *Nat. Mater.* **11**, 44–48 (2011).

28 Li, W., Hendriks, K. H., Furlan, A., Wienk, M. M. & Janssen, R. A. High quantum efficiencies in polymer solar cells at energy losses below 0.6 eV. *J. Am. Chem. Soc.* **137**, 2231–2234 (2015).

29 Meng, D. *et al.* High-performance solution-processed non-fullerene organic solar cells based on selenophene-containing perylene bisimide acceptor. *J. Am. Chem. Soc.* **138**, 375–380 (2016).

30 Zhang, J. *et al.* Ring-fusion of perylene diimide acceptor enabling efficient nonfullerene organic solar cells with a small voltage loss. *J. Am. Chem. Soc.* **139**, 16092–16095 (2017).

31 Holliday, S. *et al.* High-efficiency and air-stable P3HT-based polymer solar cells with a new non-fullerene acceptor. *Nat. Commun.* **7**, 11585 (2016).

32 Baran, D. *et al.* Reducing the efficiency–stability–cost gap of organic photovoltaics with highly efficient and stable small molecule acceptor ternary solar cells. *Nat. Mater.* **16**, 363–369 (2017).

33 Baran, D. *et al.* Reduced voltage losses yield 10% efficient fullerene free organic solar cells with > 1 V open circuit voltages. *Energy Environ. Sci.* **9**, 3783–3793 (2016).

34 Lin, Y. *et al.* An electron acceptor challenging fullerenes for efficient polymer solar cells. *Adv. Mater.* **27**, 1170–1174 (2015).

35 Zhao, W. *et al.* Molecular optimization enables over 13% efficiency in organic solar cells. *J. Am. Chem. Soc.* **139**, 7148–7151 (2017).

36 Zhang, H. *et al.* Over 14% Efficiency in organic solar cells enabled by chlorinated nonfullerene small-molecule acceptors. *Adv. Mater.* **30**, 1800613 (2018).

37 Yuan, J. *et al.* Single-junction organic solar cell with over 15% efficiency using fused-ring acceptor with electron-deficient core. *Joule* **3**, 1140–1151 (2019).

38 Cui, Y. *et al.* Over 16% efficiency organic photovoltaic cells enabled by a chlorinated acceptor with increased open-circuit voltages. *Nat. Commun.* **10**, 2515 (2019).

39 Kim, K.-H. & Kim, J.-J. Origin and control of orientation of phosphorescent and TADF dyes for high-efficiency OLEDs. *Adv. Mater.* **30**, 1705600 (2018).

40 Jurow, M. J. *et al.* Understanding and predicting the orientation of heteroleptic phosphors in organic light-emitting materials. *Nat. Mater.* **15**, 85–91 (2015).

41 Schmidt, T. D. *et al.* Emitter orientation as a key parameter in organic light-emitting diodes. *Phys. Rev. Appl.* **8**, 037001 (2017).

42 Moon, C.-K., Kim, K.-H. & Kim, J.-J. Unraveling the orientation of phosphors doped in organic semiconducting layers. *Nat. Commun.* **8**, 791 (2017).

43 Lee, J. *et al.* Deep blue phosphorescent organic light-emitting diodes with very high brightness and efficiency. *Nat. Mater.* **15**, 92–98 (2016).

44 Tuong Ly, K. *et al.* Near-infrared organic light-emitting diodes with very high external quantum efficiency and radiance. *Nat. Photonics* **11**, 63–68 (2016).

45 Uoyama, H., Goushi, K., Shizu, K., Nomura, H. & Adachi, C. Highly efficient organic light-emitting diodes from delayed fluorescence. *Nature* **492**, 234–238 (2012).

46 Hirata, S. *et al.* Highly efficient blue electroluminescence based on thermally activated delayed fluorescence. *Nat. Mater.* **14**, 330–336 (2014).

47 Zhang, Q. *et al.* Efficient blue organic light-emitting diodes employing thermally activated delayed fluorescence. *Nat. Photonics* **8**, 326–332 (2014).

48 Lin, T.-A. *et al.* Sky-blue organic light emitting diode with 37% external quantum efficiency using thermally activated delayed fluorescence from spiroacridine–triazine hybrid. *Adv. Mater.* **28**, 6976–6983 (2016).

49 Kaji, H. *et al.* Purely organic electroluminescent material realizing 100% conversion from electricity to light. *Nat. Commun.* **6**, 8476 (2015).

50 Zeng, W. *et al.* Realizing 22.5% external quantum efficiency for solution-processed thermally activated delayed-fluorescence OLEDs with red emission at 622 nm via a synergistic strategy of molecular engineering and host selection. *Adv. Mater.* **31**, 1901404 (2019).

51 Wong, M. Y. & Zysman-Colman, E. Purely organic thermally activated delayed fluorescence materials for organic light-emitting diodes. *Adv. Mater.* **29**, 1605444 (2017).

52 Dias, F. B. *et al.* The role of local triplet excited states and D–A relative orientation in thermally activated delayed fluorescence: photophysics and devices. *Adv. Sci.* **3**, 1600080 (2016).

53 Etherington, M. K., Gibson, J., Higginbotham, H. F., Penfold, T. J. & Monkman, A. P. Revealing the spin–vibronic coupling mechanism of thermally activated delayed fluorescence. *Nat. Commun.* **7**, 13680 (2016).

54 Samanta, P. K., Kim, D., Coropceanu, V. & Brédas, J.-L. Up-conversion intersystem crossing rates in organic emitters for thermally activated delayed fluorescence: impact of the nature of singlet vs triplet excited states. *J. Am. Chem. Soc.* **139**, 4042–4051 (2017).

55 Noda, H. *et al.* Critical role of intermediate electronic states for spin-flip processes in charge-transfer-type organic molecules with multiple donors and acceptors. *Nat. Mater.* **18**, 1084–1090 (2019).

56 Nakanotani, H. *et al.* High-efficiency organic light-emitting diodes with fluorescent emitters. *Nat. Commun.* **5**, 4016 (2014).

57 Pershin, A. *et al.* Highly emissive excitons with reduced exchange energy in thermally activated delayed fluorescent molecules. *Nat. Commun.* **10**, 597 (2019).

58 Hatakeyama, T. *et al.* Ultrapure blue thermally activated delayed fluorescence molecules: efficient HOMO–LUMO separation by the multiple resonance effect. *Adv. Mater.* **28**, 2777–2781 (2016).

59 Kondo, Y. *et al.* Narrowband deep-blue organic light-emitting diode featuring an organoboron-based emitter. *Nat. Photonics* **13**, 678–682 (2019).

60 Di, D. *et al.* High-performance light-emitting diodes based on carbene-metal-amides. *Science* **356**, 159–163 (2017).

61 Hamze, R. *et al.* Eliminating nonradiative decay in Cu(I) emitters: > 99% quantum efficiency and microsecond lifetime. *Science* **363**, 601–606 (2019).

62 Freeman, D. M. E. *et al.* Synthesis and exciton dynamics of donor-orthogonal acceptor conjugated polymers: reducing the singlet–triplet energy gap. *J. Am. Chem. Soc.* **139**, 11073–11080 (2017).

63 Schweicher, G. et al. Chasing the 'killer' phonon mode for the rational design of low disorder, high mobility molecular semiconductors. *Adv. Mater.* **31**, 1902407 (2019).

64 Rivnay, J. *et al.* Structural control of mixed ionic and electronic transport in conducting polymers. *Nat. Commun.* **7**, 11287 (2016).

65 Someya, T., Bao, Z. & Malliaras, G. G. The rise of plastic bioelectronics. *Nature* **540**, 379–385 (2016).

66 Giovannitti, A. *et al.* Controlling the mode of operation of organic transistors through side-chain engineering. *Proc. Natl Acad. Sci. USA* **113**, 12017–12022 (2016).

67 Nielsen, C. B. *et al.* Molecular design of semiconducting polymers for high-performance organic electrochemical transistors. *J. Am. Chem. Soc.* **138**, 10252–10259 (2016).

68 Leeuw, D. M. d., Simenon, M. M. J., Brown, A. R. & Einerhand, R. E. F. Stability of n-type doped conducting polymers and consequences for polymeric microelectronic devices. *Synth. Met.* **87**, 53–59 (1997).

69 Giovannitti, A. *et al.* N-type organic electrochemical transistors with stability in water. *Nat Commun* **7**, 13066 (2016).

70 Sun, H. *et al.* Complementary logic circuits based on high-performance n-type organic electrochemical transistors. *Adv. Mater.* **30**, 1704916 (2018).

71 Yao, H. *et al.* 14.7% Efficiency organic photovoltaic cells enabled by active materials with a large electrostatic potential difference. *J. Am. Chem. Soc.* **141**, 7743–7750 (2019).

72 Peng, Q., Obolda, A., Zhang, M. & Li, F. Organic light-emitting diodes using a neutral π radical as emitter: the emission from a doublet. *Angew. Chem. Int. Ed.* **54**, 7091–7095.
73 Ai, X. *et al.* Efficient radical-based light-emitting diodes with doublet emission. *Nature* **563**, 536–540 (2018).
74 Nagata, R., Nakanotani, H., Potscavage Jr, W. J. & Adachi, C. Exploiting singlet fission in organic light-emitting diodes. *Adv. Mater.* **30**, 1801484 (2018).
75 Salehi, A. *et al.* Realization of high-efficiency fluorescent organic light-emitting diodes with low driving voltage. *Nat. Commun.* **10**, 2305 (2019).
76 Kimura, K. *et al.* Selective triplet exciton formation in a single molecule. *Nature* **570**, 210–213 (2019).
77 Di, D. *et al.* Efficient triplet exciton fusion in molecularly doped polymer light-emitting diodes. *Adv. Mater.* **29**, 1605987 (2017).
78 Onwubiko, A. *et al.* Fused electron deficient semiconducting polymers for air stable electron transport. *Nat. Commun.* **9**, 416 (2018).

[H1] Acknowledgements

B.S. acknowledges the UK Research and Innovation for Future Leaders Fellowship no. MR/S031952/1 and the British Council no. 337323.

[H1] Author contributions

All authors contributed equally to the preparation of this manuscript.

[H1] Competing interests statement

The authors declare no competing interests.

[H1] Publisher's note

Springer Nature remains neutral with regard to jurisdictional claims in published maps and institutional affiliations.

[H1] How to cite this article

Bronstein, H., Nielsen, C. B., Schroeder, B. C. & McCulloch, I. The role of chemical design on the performance of organic semiconductors. *Nat. Rev. Chem.* **4**, xxxxx (2020).

[H1] ToC blurb

[insert 25 word summary]

Subject terms

Conjugated polymers URI /639/638/455/954

Electronic materials URI /639/638/298/917

Photochemistry URI /639/638/439